Mechanical Properties of Lightweight Cellular Concrete for Geotechnical Applications

Binod Tiwari, M.ASCE[1]; Beena Ajmera, A.M.ASCE[2]; Ryan Maw, M.ASCE[3]; Ryan Cole, M.ASCE[4]; Diego Villegas[5]; and Peter Palmerson[6]

Abstract: Lightweight cellular concrete provides many advantages in geotechnical applications, however, its use has been limited because of a lack of understanding of its engineering properties. In this study, laboratory soil tests were conducted on lightweight cellular concrete having four different densities, and shear strength parameters, coefficients of permeability, and at-rest earth pressure coefficients were measured. Unconfined compressive strength and as undrained strength properties (total friction angle and cohesion intercept) of partially saturated materials were found to be dependent on the density of the lightweight cellular concrete specimen. However, the effective friction angle and cohesion intercept of the saturated materials were independent of the test unit weight over the range of stresses tested. The effective friction angle and cohesion values of the lightweight cellular concrete materials, determined from direct simple shear tests, were 35° and 36 kPa, respectively. Back-pressure saturated samples from isotropically consolidated drained and isotropically consolidated undrained triaxial tests yielded an effective friction angle of 34° and a cohesion intercept of 78 kPa, similar to the results obtained from the constant-volume direct simple shear tests. The at-rest earth pressure coefficient was found to range between 0.2 and 0.5, while Poisson's ratio for these materials was observed to range between 0.20 and 0.30. Recommendations are made for appropriate geotechnical engineering properties for the use of lightweight cellular concrete materials in earth-retaining structures. **DOI: 10.1061/(ASCE)MT.1943-5533.0001885.** *This work is made available under the terms of the Creative Commons Attribution 4.0 International license, http://creativecommons.org/licenses/by/4.0/.*

Downloaded from ascelibrary.org by 173.10.17.45 on 08/30/17. Copyright ASCE. For personal use only; all rights reserved.

Background

Lightweight concrete has been implemented in civil engineering construction for approximately 3,000 years, with the use of volcanic ash as a fine aggregate (Maruyama and Camarini 2015; Chandra and Berntsson 2003). Advances in technology and new materials have led to advancements in strength, durability, and production consistency. Today, lightweight cellular concrete (LCC) is gaining popularity in many construction applications such as to reduce earth pressures, minimize dynamic forces, mitigate settlement, and absorb earthquake forces in subsurface structures. As a result of these new applications, a better understanding is needed regarding the engineering properties of these materials.

The vesicular structure of LCC is obtained when air bubbles develop in a cement paste by stirring in water and proprietary admixtures (Maruyama and Camarini 2015). LCC poses a number of benefits, such as high durability, noncorrosivity, permanence, lightweight density, high freeze-thaw resistivity, and low permeability, low water absorption capacity, and it provides high damping against dynamic loads. In addition, LCC provides a more economical alternative than traditional methods for reducing loads on different infrastructure (Maruyama and Camarini 2015; Tikalsky et al. 2004; LaVallee 1999; Aberdeen Group 1963).

Several researchers have examined different properties of LCC including thermal conductivity (Neville 2002; Loudon 1979; Aberdeen Group 1963), drying shrinkage (Aberdeen Group 1963; Narayanan and Ramamurthy 2000), and thermal expansion (Aberdeen Group 1963). Narayanan and Ramamurthy (2000) found that the unconfined compressive strength (UCS) of LCC increases linearly with an increase in density and inversely with an increase in moisture content. LaVallee (1999) and Zaidi et al. (2008) also reported values for the UCS. Compressive strength values can vary substantially based on the foaming agent used when preparing the LCC (Aberdeen Group 1963).

Many of the mechanical properties of LCC are currently unknown; an understanding of these properties is necessary in order to appropriately incorporate LCC into geotechnical applications. In this study, UCS, total and effective shear strength parameters, consolidation characteristics, at-rest earth pressure (K_o) coefficients, hydraulic conductivity, and Poisson's ratio values were measured for LCC samples prepared at four different test densities. Using this information, recommendations for design of the backfill of mechanically stabilized earth (MSE) walls using LCC are provided.

Materials and Methods

LCC Casting and Curing

The LCC used in this study was prepared using two concurrent processes. In the first of these, one part Elastizell Foam Concentrate, a protein-based biodegradable surfactant by-product of the

[1]Professor, Dept. of Civil and Environmental Engineering, California State Univ., Fullerton, 800 N State College Blvd., E-419, Fullerton, CA 92834. E-mail: btiwari@fullerton.edu

[2]Assistant Professor, Dept. of Civil and Environmental Engineering, California State Univ., Fullerton, 800 N State College Blvd., E-318, Fullerton, CA 92834 (corresponding author). E-mail: bajmera@fullerton.edu

[3]Project Engineer, Gerhart Cole, Inc., 668 E 12225 S, Suite 203, Draper, UT 84020. E-mail: ryanm@gerhartcole.com

[4]Principal, Gerhart Cole, Inc., 668 E 12225 S, Suite 203, Draper, UT 84020. E-mail: ryan@gerhartcole.com

[5]Engineer, Cell Crete Corporation, 135 E Railroad Ave., Monrovia, CA 91016. E-mail: dvillegas@cell-crete.com

[6]Geotechnical Engineer, Cell Crete Corporation, 135 E Railroad Ave., Monrovia, CA 91016. E-mail: ppalmerson@cell-crete.com

Note. This manuscript was submitted on January 27, 2016; approved on November 4, 2016; published online on March 2, 2017. Discussion period open until August 2, 2017; separate discussions must be submitted for individual papers. This technical note is part of the ***Journal of Materials in Civil Engineering***, © ASCE, ISSN 0899-1561.

food industry (EF 2015), was added to forty parts (1:40) water. The concentrate and water mixture were mechanically agitated through a small nozzle to produce a foam and subjected to compressed air action at a high pressure. Simultaneously, cement and water were mixed together using a specific mix design. The mixing occurred in a customized concrete mixer that was coupled with a progressing cavity pump. A volumetric blending system was used to merge the cement and water to produce the neat cement slurry, which was then pumped into a proprietary blending system where the preformed foam was introduced. This introduction produces an air-filled cellular concrete whose density is dependent on the ratio of foam and neat cement grout. Samples were cured in a moisture- and temperature-controlled environment, following the curing process outlined in ASTM C495/C495M-12 (ASTM 2012).

For each specimen tested, three different unit weight values were determined: (1) unit weight of the specimen prior to trimming, (2) test unit weight, and (3) dry unit weight of the specimen after it was oven-dried for at least 24 h. The unit weights prior to trimming ranged from 3.1 to 3.8 kN/m^3, 3.4 to 4.7 kN/m^3, 4.4 to 6.1 kN/m^3, 3.8 to 6.6 kN/m^3, and 4.9 to 7.5 kN/m^3 for Class II, Batch 1; Class II,Batch 2; Class IV; 7.1 kN/m^3 cast unit weight; and 8.6 kN/m^3 cast unit weight LCC samples. Similarly, the test unit weight ranged from 3.0 to 3.8 kN/m^3, 3.3 to 5.0 kN/m^3, 4.5 to 5.4 kN/m^3, 5.0 to 6.8 kN/m^3, and 5.1 to 7.5 kN/m^3, respectively. The maximum cast unit weight was used to separate the four classes of LCC materials. The class definitions suggested in Caltrans (2013) were adopted in this study. The dry unit weight was not measured in the Class-II Batch-1 specimens, but ranged from 2.3 to 3.6 kN/m^3, 3.3 to 4.3 kN/m^3, 4.4 to 5.8 kN/m^3, and 4.4 to 6.1 kN/m^3, respectively, for the remaining LCC batches.

Unconfined Compression Strength Test

Shear strength testing was performed on all of the LCC batches to characterize drained and undrained strength behavior. A strain rate of 0.5%/h, following the recommendations in ASTM D2166-00 (ASTM 2000), was selected. Shearing continued until the peak strength was measured. If the peak strength was not achieved by 15% axial strain, testing was terminated. The specimen was then removed from the apparatus and placed in an oven to dry for 24 h in order to measure its moisture content and determine its dry unit weight.

Direct Shear Test

The DS test was conducted in accordance to ASTM D3080-11 (ASTM 2011c). The moist (partially saturated) specimens were first consolidated to the desired stress. Because the samples were partially saturated, the term *consolidation* is not appropriate for this type of DS testing. However, because a standard is not available for the DS test of partially saturated soils, and to follow the ASTM procedure for saturated soils, the term *consolidation* is used in this paper to refer to vertical deformation under a static vertical stress prior to application of shear stress. The shearing rates were set based on the results obtained through vertical deformation time data following the ASTM procedure. The strength measured with the DS testing was considered total stress in this study. In this study, a specimen was consolidated to a stress of 25 kPa, three each to stresses of 50, 75, and 100 kPa, one specimen to a stress of 200 kPa, and one specimen to a stress of 350 kPa. The primary consolidation was monitored with the use of a real-time computer-generated logarithm of time versus deformation curves. Once the primary consolidation was complete, the specimen was sheared at a rate of 0.1 mm/min, which was the fastest shearing rate determined from the consolidation data using ASTM D3080-11, assuming that the peak shear stress would occur at 1 mm shear displacement, until the peak strength was measured. If the peak strength was not obtained within 7 mm of horizontal displacement, the test was terminated at that point. After the shearing phase, the specimen was removed from the DS box and placed in an oven for at least 24 h to measure the moisture content and determine the dry unit weight of the specimen.

Direct Simple Shear Test

DSS tests were conducted using a Norwegian Geotechnical Institute (NGI) device (Bjerrum and Landva 1966; Dyvik et al. 1987). In this device, the sample was consolidated to the desired stress. For each batch, a total of 11 static DSS tests at four different consolidation stresses were performed. Specifically, three samples were each consolidated to a stress of 25, 50, and 100 kPa, and two samples were consolidated to a stress of 350 kPa. A real-time relationship between the logarithm of time and the vertical deformation was monitored to determine the completion of primary consolidation, at which point, the specimens were subjected to undrained strain-controlled shearing at a rate of 5%/h, as recommended in ASTM D6528-07 (ASTM 2007). The shearing phase was continued until the peak shear strength was measured or a maximum of 25% shear strain was reached. The specimen was then removed from the apparatus and placed in an oven for at least 24 h to determine the moisture content and dry unit weight.

The majority of LCC specimens were back-pressure saturated using a permeameter connected to the sample, with cell pressure applied using a triaxial test assembly. The saturated sample was used to conduct a static DSS test using the process previously described. The sample was submerged in water as soon as it was removed from the permeameter and during sample preparation and testing. Several LCC samples were also tested without back-pressure saturation and tested in the moist condition. The effective shear strength parameters obtained from the saturated specimens were similar to those obtained from the partially saturated (i.e., moist) specimens. The advantage of the constant-volume DSS device used in this study is that the partially saturated specimens yielded results equivalent to those for the saturated specimens.

Isotropically Consolidated Drained and Isotropically Consolidated Undrained Triaxial Tests

Triaxial shear strength testing was performed on cured, continuous (no visible cracks) LCC to characterize drained and undrained shear strengths. The range of the B values varied between samples tested and reached up to 0.94. The loading rate was calculated using both guidance provided by Bishop and Henkel (1967) from measured rates during consolidation and observations during testing. Isotropically consolidated drained (CID) triaxial testing was performed in general accordance with ASTM D7181-11 (ASTM 2011a) and Bureau of Reclamations Standard USBR 5755 (USBR 1990). Similarly, isotropically consolidated undrained (CIU) triaxial testing was performed in general accordance with ASTM D4767-11 (ASTM 2011b) and USBR 5750 (USBR 1990). Method A was selected to estimate the effective area of consolidated samples. Given the vesicular nature of the samples, no filter paper was used in sample preparation. Double membranes were used in testing, and appropriate corrections were applied to the testing results.

K_o Consolidation

The K_o consolidation triaxial testing was performed to measure Poisson's ratio and at-rest or K_o lateral stresses developed through consolidation by adjusting the lateral stresses to maintain no radial

Downloaded from ascelibrary.org by 173.10.17.45 on 08/30/17. Copyright ASCE. For personal use only; all rights reserved.

volume change. Sample testing consisted of axial loading applied by the triaxial piston with an automated program, *TruePath* (Geotac 2005), adjusting the cell pressure to match the horizontal pressure transfer from sample consolidation. The automated balancing of cell pressure provided a direct measurement of the at-rest horizontal pressure of the tested sample under axial loading. The K_o consolidation testing was performed using USBR 5740-89 (USBR 1990).

Hydraulic Conductivity

Hydraulic conductivity testing was performed using a flexible wall (i.e., membrane) and a triaxial cell in accordance with Method C of ASTM 5084-10 (ASTM 2010). The hydraulic conductivity testing included double membranes on the sample. An appreciable change in measured hydraulic conductivity values as a result of different confining stresses was not observed. The change in hydraulic conductivity did not appear to change with the amount of pore volumes of water tested through the samples.

One-Dimensional Consolidation

One-dimensional (1D) consolidation testing was performed for a comparison with K_o loading and material behavior from one ID and triaxial loadings. Additionally, 1D consolidation testing was performed to measure the sensitivity of the sample to yielding and settlement versus axial loading following ASTM D2435/D2435M-11 (ASTM 2011d) and USBR 5700 (USBR 1990).

Results and Discussion

UC Test

Visual inspection of the LCC samples revealed that the vesicular sections of cellular concrete were crushed under unconfined compression (UC) loads. Failure initiated with the development of vertical cracks; with continued application of axial strain, pieces of LCC material would break away from the specimen along the radial directions. For concrete cylinders, this type of failure mode would be described as columnar, defined according to ASTM C39-15 (ASTM 2015). Pictures of failed specimens are available in Tiwari (2016).

For each group of specimens tested, the typical stress-strain curves obtained from the UC tests are shown in Fig. 1. Ductile behavior was observed in the Class-II and Class-IV specimens tested, whereas the specimens with cast unit weights of 7.1 and 8.6 kN/m^3 tended to exhibit more brittle behavior. Specifically, an increase in material unit weight resulted in an increase in peak strength. A decrease in the strain required to reach this peak strength as the test unit weight of the LCC specimens increased was also noted.

Fig. 1 shows that a typical curve of the UCS of LCC is dependent on the unit weight of the specimen tested. Fig. 2 shows the relationship between the test unit weight and the measured UCS. The results are presented separately for each batch tested. An increase in the air volumes present in lighter samples (samples with lower test unit weights) in comparison with the denser samples resulted in a decreased UCS. Thus, as shown in Fig. 2, as the test unit weight of the specimen decreases, the UCS also decreases. A best-fit polynomial regression line relating the UCS to the test unit weight is also shown in Fig. 2. The equation for the regression line is provided in Eq. (1), where *UCS* is the unconfined compressive strength in kPa and γ is the test unit weight in kN/m^3. The coefficient of determination of this regression line is 0.94. Lines

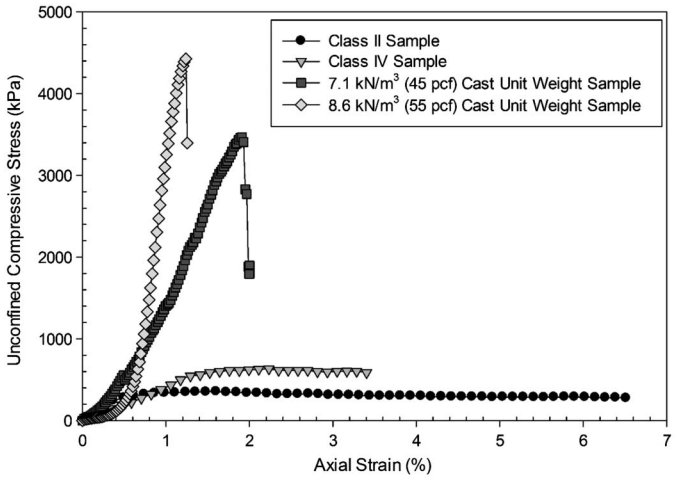

Fig. 1. Typical stress-strain curves from the UC test

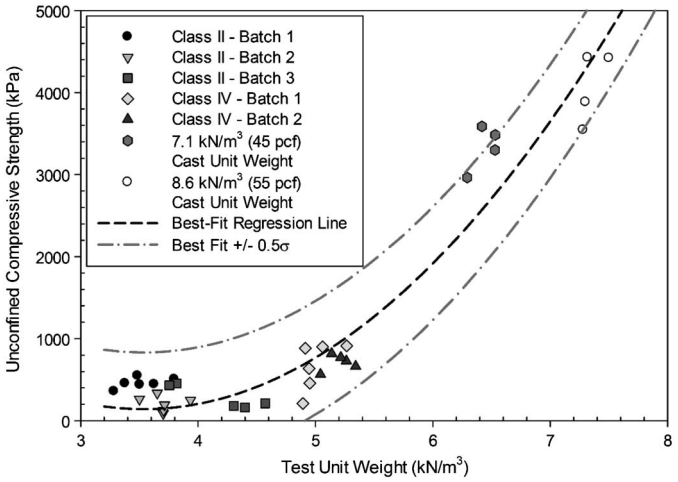

Fig. 2. Relationship between unconfined compressive strength of LCC specimens with their corresponding test unit weights

representing ± 0.5 standard deviations (σ) from the best-fit regression are also shown in Fig. 2. All of the data, except one point, were observed to lie within the bounds established by these lines.

$$UCS = 291.98\gamma^2 - 2063.4\gamma + 3785 \quad (1)$$

DS Test

Fig. 3 shows the shear stress versus horizontal displacement behavior of the LCC specimens at four normal stresses, as obtained from the DS tests. The results are for the LCC batch with a cast unit weight of 7.1 kN/m^3. The shear stress versus horizontal displacement was similar in all LCC specimens tested and are available in Tiwari (2016). Presented in Fig. 4 are the Mohr-Coulomb failure envelopes obtained from the DS tests. As can be seen, an increase in the test unit weight of the specimens results in a significant increase in the cohesion intercept and a slight increase in the total friction angle of the LCC specimens. Notably, the term *total friction angle* used in this study corresponds to the friction angle of partially saturated LCC specimens obtained from the DS tests

Downloaded from ascelibrary.org by 173.10.17.45 on 08/30/17. Copyright ASCE. For personal use only; all rights reserved.

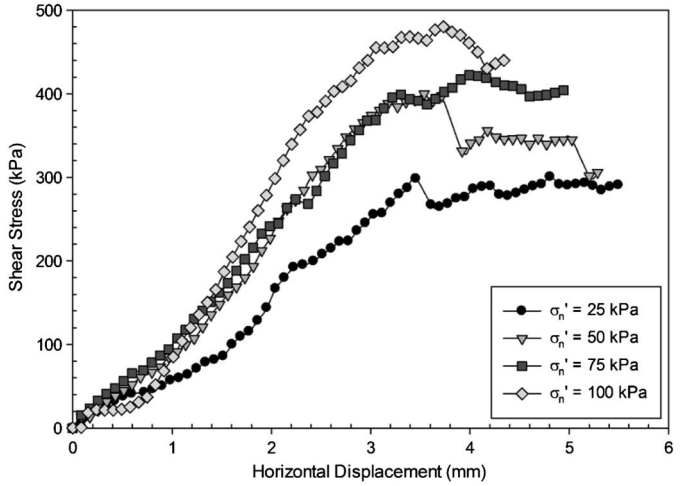

Fig. 3. Shear stress versus horizontal displacement from the DS tests on LCC specimens with a cast unit weight of 7.1 kN/m^3 at four normal stresses

performed at the shearing rate specified earlier. Eq. (2) can be used to estimate the total friction angle (φ), in degrees, of the specimen using the average test unit weight (γ), given in kN/m^3. The coefficient of determination for Eq. (2) is 0.91. The relationship between the cohesion and average test unit weight is given by Eq. (3), which has a coefficient of determination of 0.60. The average test unit weight (γ) is expressed in kN/m^3 and the cohesion in kPa

$$\varphi = 1.187\gamma + 15.062 \tag{2}$$

$$c = 274.386\gamma - 654.958 \tag{3}$$

DSS Test

Typical curves for shear stress versus shear strain and pore water pressure versus shear strain obtained from the constant-volume DSS test are shown in Fig. 5, which contains the results for a Class-II Batch-2 sample at a consolidation pressure of 100 kPa. The response observed in all LCC specimens was similar and can be found in Tiwari (2016). An increase in the normal stress corresponded to an increase in the shear stress and a decrease in the shear strain required to achieve the peak strength. Similarly, the peak shear stress increased as the test unit weight of the LCC specimens increased. The shear strain required to reach the peak strength decreased as the test unit weight increased.

The relationship between the undrained strength ratios, defined as shear strength normalized by consolidation pressure, and the consolidation pressure of the tested LCC materials is shown in Fig. 6, where the value of the undrained strength ratio does not decrease significantly when the consolidation pressure exceeds approximately 150 kPa. The LCC materials with lower test unit weights tend to have slightly lower undrained strength ratios at the same consolidation pressure compared with the materials with higher test unit weights. The effective stress failure envelope is shown in Fig. 7, where the effect of the test unit weight of the LCC is eliminated by examining the effective stress results obtained in the DSS device. The effective friction angle was computed to be 35° with the cohesion intercept equal to 36 kPa. Lines representing ± 0.5 standard deviation (σ) from the failure envelope are also included in the figure. As can be observed, all of the data points obtained fell within these bounds.

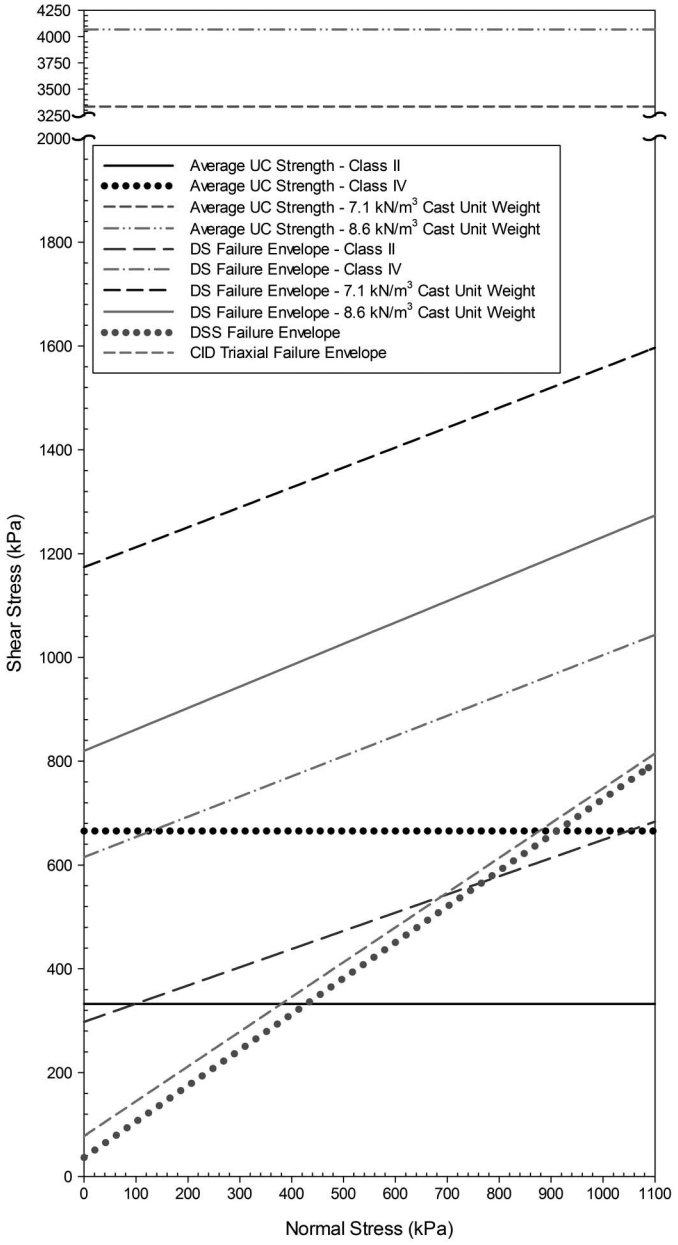

Fig. 4. Average shear envelopes of all sample types obtained from the DS, DSS, and CID triaxial tests

CID and CIU Tests

Typical CID and CIU test results for the Class-II and Class-IV LCC samples are shown in Fig. 8. The were converted into a shear envelope and exhibited a cohesion intercept of 78 kPa and an effective friction angle of 34°, as shown in Fig. 4. This effective friction angle compares well with the results obtained from the DSS test, which is explained later.

K_o Consolidation

A summary of the measured K_o for two of the Class-II and Class-IV LCC samples are provided in Fig. 9. These plotted test results provide a comparison of the measured K_o pressures for the two LCC classes. As can be observed in Fig. 9, the K_o values ranged from approximately 0.4 to 0.5 for Class-II and from 0.2 to 0.3 for Class-IV. Also, as the test unit weight of the material increases K_o is found to decrease. Moreover, K_o decreases from 1.6 to the values

Downloaded from ascelibrary.org by 173.10.17.45 on 08/30/17. Copyright ASCE. For personal use only; all rights reserved.

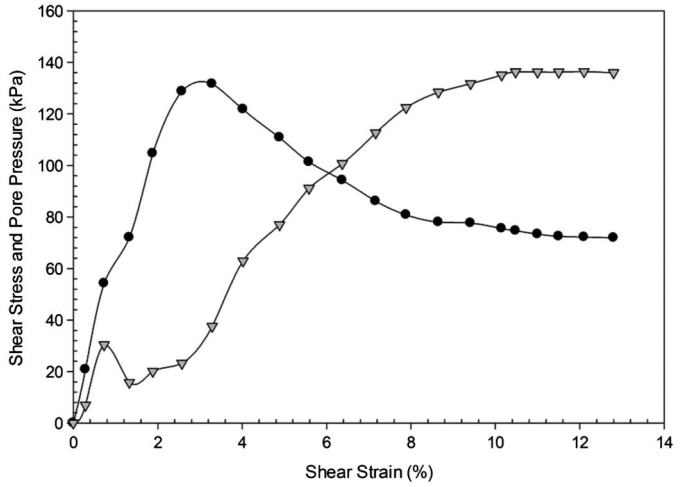

Fig. 5. Typical shear stress and pore pressure response with shear strain observed in the DSS device (presented here for the Class-II Batch-2 specimen at 100-kPa consolidation pressure)

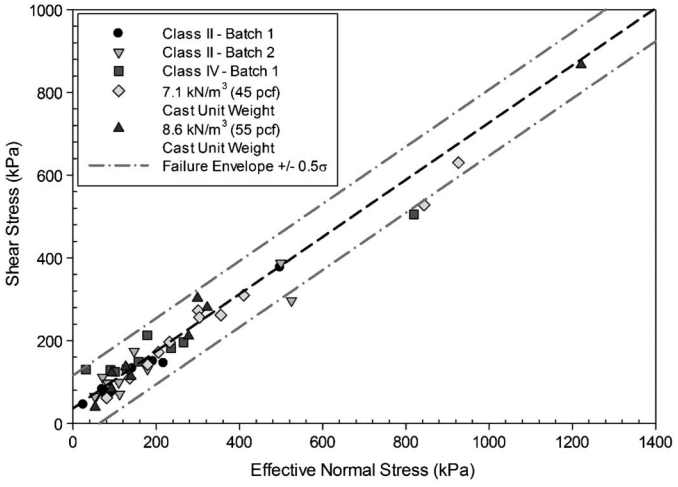

Fig. 7. Effective stress failure envelope obtained from the DSS tests for LCC specimens

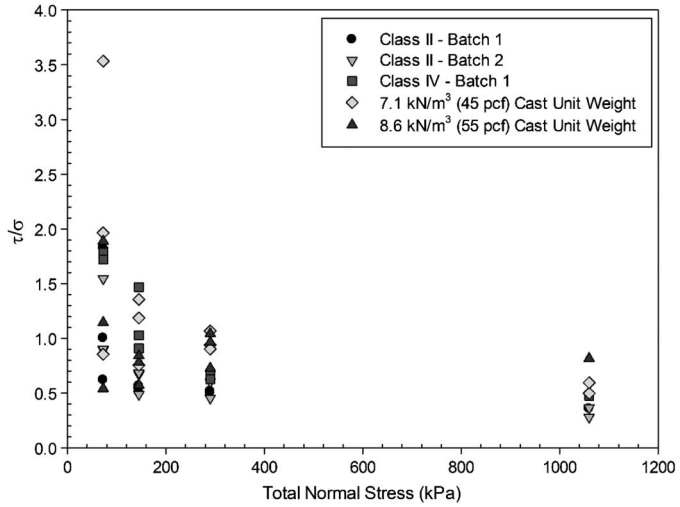

Fig. 6. Relationship between undrained strength ratio and consolidation pressure obtained from the DSS tests for LCC specimens

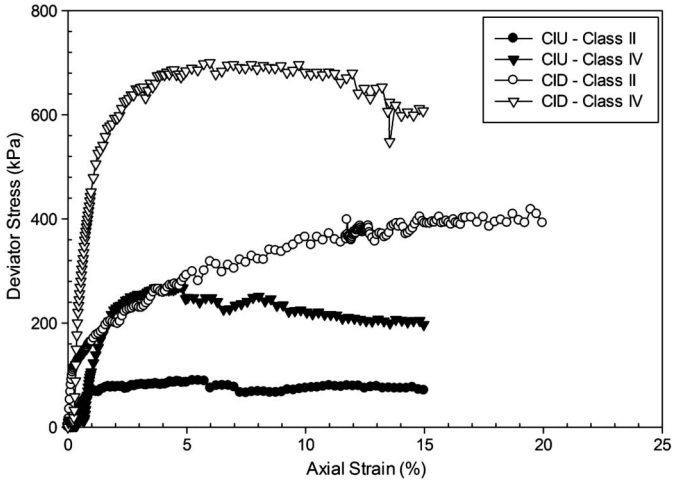

Fig. 8. Typical CID and CIU test results for Class-II and Class-IV LCC materials obtained at 86.2-kPa cell pressure

noted previously for an increase in major principal stress from approximately 10 to 150 kPa and remained more or less constant for higher major principal stresses. In Fig. 9, the lower value of K_o is observed after exceeding small axial strains.

Poisson's ratios relative to the major principal stress and axial strain are also shown in Fig. 9 for both Class-II and Class-IV LCC samples. The test results show a horizontal pressure exerted from the sample under axial loading and variation in the ratio of lateral transfer based on loading conditions. As can be observed, the Poisson's ratio generally ranges from 0.20 to 0.30.

1D Consolidation

A summary of the consolidation results for the Class-II and Class-IV LCC samples is shown in Fig. 10, where the test results indicate a notable difference in the elastic behavior of the two classes of cellular concrete. Class-IV specimens yield at a higher pressure with a lower deformation under higher vertical stresses. Also, Class-II and Class-IV LCC materials exhibit compressive

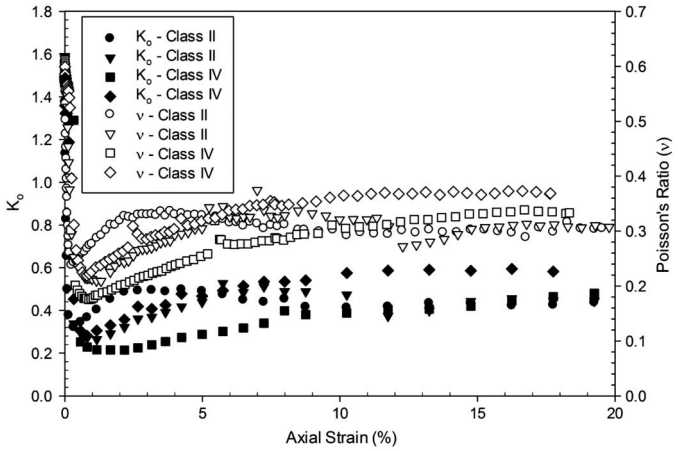

Fig. 9. Variation in K_o and Poisson's ratio with axial strain

Downloaded from ascelibrary.org by 173.10.17.45 on 08/30/17. Copyright ASCE. For personal use only; all rights reserved.

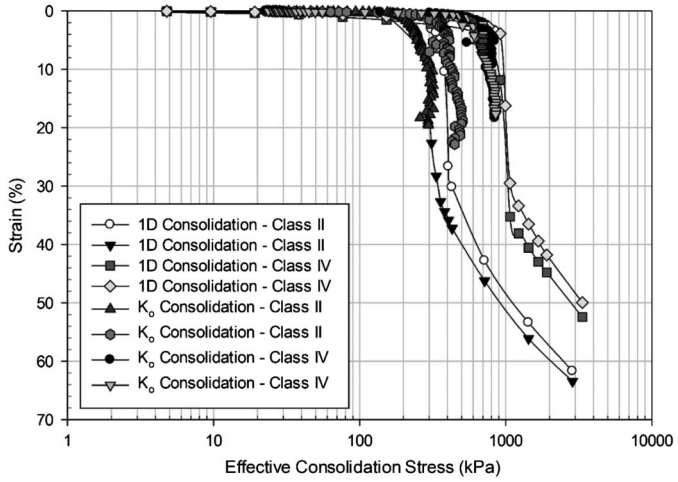

Fig. 10. Summary of consolidation test results for Class-II and Class-IV samples

behavior similar to that of soil specimens preconsolidated to equivalent pressures of 300 and 700 kPa, respectively.

The K_o consolidation test data are plotted in Fig. 10 to compare the consolidation curves developed from triaxial loading with that of one-dimensional loading. As can be seen, a reasonable agreement between K_o consolidation and 1D consolidation obtains under lower stresses, but the results diverge at higher stresses. The range over which the data appear to match between the two tests indicates that under lower loading pressures and strains/deformation, K_o pressures are more consistent but at higher strains variability in those parameters may increase. As Fig. 10 shows, the samples exhibit significant strain for vertical stresses higher than 300 and 700 kPa for Class-II and Class-IV materials, respectively.

Permeability

Reported values of hydraulic conductivity have ranged significantly with historic data on the order of 10^{-6} cm/s (Soil Exploration Company 1981). Additional guidance provided by the U.S. Army Corps of Engineers (USACE 1996) cites typical values in the range of 10^{-4} to 10^{-5} cm/s. In this study, the measured hydraulic conductivity ranged from 1.7×10^{-4} to 7.7×10^{-4} cm/s in the Class-II specimens and from 9.5×10^{-4} to 1.2×10^{-3} cm/s in the Class-IV specimens. Given the variability in referenced hydraulic conductivity, the limited data, and the historic nature of the testing, additional hydraulic conductivity testing is recommended for future use.

Application of LCC in Geotechnical Applications

Recommended Mechanical Properties of LCC for Design

Presented in Fig. 4 are the combined results that show the average shear strength of LCC materials of different unit weights tested under different conditions. As can be observed, results obtained from the CID triaxial tests are plotted between the shear envelopes obtained with DSS and DS devices. Direct shear samples exhibit high cohesion values mainly due to the apparent cohesion resulting from suction in the partially saturated material. Unfortunately, the suction values could not be measured using the existing experimental setup. The shear envelope obtained with the DSS device represents the shear strength of saturated LCC samples, as a result of the sample preparation sequence outlined previously. Moreover, DSS test results for samples with different unit weights and different degrees of saturation were plotted around a single shear envelope. Therefore, the effective friction angle obtained from the DSS test, which provided the conservative value (i.e., the value for the saturated condition) can be considered for design of engineering structures with or on the tested LCC materials. The at-rest earth pressure, obtained from the K_o consolidation tests, ranged from 0.2 to 0.5. Using the effective friction angle of 35°, obtained from the constant-volume DSS test, the calculated at-rest earth pressure coefficient, using Jaky (1944), was close to the upper limit of the measured K_o value range. Therefore, an effective LCC friction angle of 35° for design purposes should provide a reasonably conservative estimate of the drained strength for saturated samples. However, the drained shear strength should be limited by the strengths obtained from the UC tests. Because there is only a very small possibility that LCC materials will be fully saturated under normal conditions, use of total shear strength obtained with the DS tests may also provide reasonable estimates of shear strength. The shear strength obtained with the DS tests with no cohesion led to the friction angle of 40°, which was higher than the effective friction angles obtained for saturated LCC. However, the corresponding shear strength for partially saturated LCC was higher than that for fully saturated LCC up to certain effective vertical stress and lower for effective vertical stress higher than this limiting effective vertical stress. The design friction angle may be increased up to 40° with Class-II or Class-IV LCC subjected to normal stresses lower than 400 kPa, 7.1-kN/m^3 cast unit weight LCC subjected to normal stresses less than 500 kPa, and 8.6-kN/m^3 cast unit weight LCC subjected to normal stresses less than 1,000 kPa.

Use of LCC for Backfill of Mechanically Stabilized Earth Walls

Current retaining/mechanically stabilized earth (MSE) wall design does not include cohesion because it is considered to be largely a transient property in granular materials. Therefore, it is recommended, at this stage of development, to use an effective friction angle of 35° and ignore cohesion when calculating external stability of retaining/MSE walls for long-term conditions. The effective friction angle may be increased up to 40° when Class-II or Class-IV 7.1 kN/m^3 cast unit weight and 8.6 kN/m^3 cast unit weight LCC is subjected to normal stresses less than 400, 500, and 1,000 kPa, respectively. It may be appropriate to include cohesion in temporary construction cases based on engineering judgment concerning duration and loading conditions. Although LCCs in typical wall conditions do not have a high likelihood of saturation, saturation is critical for accurate measurements of volume change for drained tests and generated pore pressures for undrained tests [ASTM STP977 (ASTM 1988)]. Given these considerations and assumptions, using the effective friction angle measured under near saturated laboratory conditions provides what is believed to be a reasonably conservative approach. The significantly higher cohesion obtained with the DS test for unsaturated LCCs indicates that LCC backfills may be temporarily freestanding and may not result in significant earth pressures under short-term conditions. However, given the potential for long-term material degradation and/or saturation under field conditions, which were outside the scope of this study, it is recommended that a traditional earth pressure approach using an effective friction angle from saturated testing (i.e., 35°) be used to evaluate the external stability of an MSE wall. This approach should also include consideration of capping or limiting strengths below ultimate values (i.e., UCS or

Downloaded from ascelibrary.org by 173.10.17.45 on 08/30/17. Copyright ASCE. For personal use only; all rights reserved.

crushing) and sensitivity of the structure to settlement deformations. Additional research should be performed to evaluate reinforcement-LCC interface shear strength for MSE wall internal stability and for external stability when Coulomb's active earth pressure coefficients are used.

The application of the material characteristics outlined here should be used only after careful consideration by an experienced design professional. A laboratory testing program using an appropriate test method (i.e., DSS, CID, CIU) should be performed for the proposed LCC mix design under project-specific conditions.

Summary and Conclusions

In order to characterize LCC materials for use in earth-retaining structures, LCC samples having of four unit weights were tested using various shear-testing devices and conditions to measure shear strength parameters, coefficients of permeability, and at-rest earth pressure coefficients. The results lead to the following conclusions:

- UCS, total friction angle and cohesion of the partially saturated LCC after 28 days of curing exhibited a strong correlation with the test unit weights;
- The effective stress failure envelopes for saturated LCC samples tested with the constant-volume DSS test exhibited an average effective friction angle of 35° and cohesion of 36 kPa;
- Results obtained from the CIU and CID triaxial tests on back-pressure saturated LCC samples exhibited an average effective friction angle of 34° and cohesion of 78 kPa, which were similar to the DSS test results; and
- The K_o values ranged from 0.2 to 0.5; the values of Poisson's ratio ranged from 0.20 to 0.30; The Class-II and Class-IV materials exhibited significant deformation at vertical stresses higher than 300 and 700 kPa, respectively.

It is recommended that cohesion be ignored and that the effective friction angle of saturated LCC (35°) be used for the materials characterized in this study. It is also suggested that external stability be evaluated using Rankine's active earth pressure because of the backfill of earth-retaining structures such as MSE walls. Interface friction between reinforcement and LCC materials along with wall-LCC materials should be measured separately for MSE wall internal stability and in case Coulomb's active earth pressure coefficients are used.

Acknowledgments

This project involved the support of many individuals and organizations. The authors appreciate the help of graduate students at California State University, Fullerton, including Miss Sneha Upadhyaya, Mr. Duc Tran, Mr. Janak Koirala, Mr. Prakash Khanal, and Miss Smriti Dhital for conducting laboratory tests and analyzing the data. Mr. Hector Zazueta's help in the test setting is also highly appreciated. The authors also recognize the observations and insights provided by Gerhart Cole, Inc., team and particularly Mr. Zach Gibbs, who primarily performed the laboratory testing at Gerhart Cole.

References

Aberdeen Group. (1963). "Cellular concrete." *Publication No. C630005*, Aberdeen Group, Boston.

ASTM. (1988). "Advanced triaxial testing of soil and rock." *ASTM STP977*, West Conshohocken, PA.

ASTM. (2000). "Standard test method for unconfined compressive strength of cohesive soil." *ASTM D2166-00*, West Conshohocken, PA.

ASTM. (2007). "Standard test method for the consolidated undrained direct simple shear testing of cohesive soils." *ASTM D6528-07*, West Conshohocken, PA.

ASTM. (2010). "Standard test methods for measurement of hydraulic conductivity of saturated porous materials using a flexible wall permeameter." *ASTM D5084-10*, West Conshohocken, PA.

ASTM. (2011a). "Method for consolidated drained triaxial compression test for soils." *ASTM D7181-11*, West Conshohocken, PA.

ASTM. (2011b). "Standard test method for consolidated undrained triaxial compression test for cohesive soils." *ASTM D4767-11*, West Conshohocken, PA.

ASTM. (2011c). "Standard test method for direct shear tests of soils under consolidated drained conditions." *ASTM D3080-11*, West Conshohocken, PA.

ASTM. (2011d). "Standard test methods for one-dimensional consolidation properties of soils using incremental loading." *ASTM D2435/D2435M-11*, West Conshohocken, PA.

ASTM. (2012). "Standard test method for compressive strength of lightweight insulating concrete." *ASTM C495/C495M*, West Conshohocken, PA.

ASTM. (2015). "Standard test method for compressive strength of cylindrical concrete specimens." *ASTM C39-15*, West Conshohocken, PA.

Bishop, A. W., and Henkel, D. J. (1967). *The measurement of soil properties in the triaxial test*, Edward Arnold Publishers, London.

Bjerrum, L., and Landva, A. (1966). "Direct simple shear tests on a Norwegian quick clay." *Geotechnique*, 16(1), 1–20.

Caltrans. (2013). "Notice to bidders and special provisions for construction on State Highway in Contra Costa County in and near Martinez from Arthur Road undercrossing to 0.5 mile north of Mococo overhead." *Project No. 0400000967*, Sacramento, CA.

Chandra, S., and Brentsson, L. (2003). *Lightweight aggregate concrete science, technology and applications*, Standard Publisher Distributors, Göteborg, Sweden.

Dyvik, R., Berre, T., Lacasse, S., and Raadim, B. (1987). "Comparison of truly undrained and constant volume direct simple shear tests." *Geotechnique*, 37(1), 3–10.

EF (Engineered Fill). (2015). "Elastizell specification section 0223." ⟨http://elastizell.com/fillspec.html⟩ (Apr. 13, 2015).

Geotac (Geotechnical Test Acquisition and Control). (2005). "TruePath version 5.4.4." Houston.

Jaky, J. (1944). "The coefficient of earth pressure at rest." *J. Soc. Hungarian Archit. Eng.*, 7, 355–358.

LaVallee, S. (1999). "Cellular concrete to the rescue." *Publication No. C99A039*, Aberdeen Group, Boston.

Loudon, A. G. (1979). "The thermal properties of lightweight cellular concretes." *Int. J. Lightweight Concr.*, 1(2), 71–85.

Maruyama, R. C., and Camarini, G. (2015). "Properties of cellular concrete for filters." *IACSIT Int. J. Eng. Technol.*, 7(3), 223–228.

Narayanan, N., and Ramamurthy, K. (2000). "Structure and properties of aerated concrete: A review." *Cem. Concr. Compos.*, 22(5), 321–329.

Neville, A. M. (2002). *Properties of concrete*, Pearson Education, Essex, U.K.

Soil Exploration Company. (1981). "Permeability tests low density Elastizell concrete cylinders." *Project No. 120–7690*, St Paul, MN.

Tikalsky, P. J., Pospisil, J., and MacDonald, W. (2004). "A method for assessment of the freeze-thaw resistance of preformed foam cellular concrete." *Cem. Concr. Res.*, 34(5), 889–893.

Tiwari, B. (2016). "Application of cell-crete in civil engineering—Phases I and II, static and dynamic properties." *Technical Rep. Project No. 50123514*.

USACE (U.S. Army Corps of Engineers). (1996). "Controlled low strength material with coal combustion ash and other recycled materials." Washington, DC.

USBR (U.S. Bureau of Reclamation). (1990). "Earth manual. Part 2." U.S. Dept. of Interior, Denver.

Zaidi, A. A. M., Rahman, A. I., and Zaidi, N. H. A. (2008). "Behavior of fiber reinforced foamed concrete: Indentation test analysis." *Proc., Seminar on Geotechnical Engineering*, Johore, Malaysia, 92–101.

Downloaded from ascelibrary.org by 173.10.17.45 on 08/30/17. Copyright ASCE. For personal use only; all rights reserved.